

Proceedings of the All-Polish Seminar on Mössbauer Spectroscopy, Warsaw, Poland, June 18–21, 2010

# Impurity Effect on Charge and Spin Density in $\alpha$ -Fe — Comparison between Cellular Model, *Ab Initio* Calculations and Experiment

A. BŁACHOWSKI<sup>a,\*</sup> AND U.D. WDOWIK<sup>b</sup>

<sup>a</sup>Mössbauer Spectroscopy Division, Institute of Physics

Pedagogical University, Podchorążych 2, PL-30-084 Kraków, Poland

<sup>b</sup>Applied Computer Science Division, Institute of Technology

Pedagogical University, Podchorążych 2, PL-30-084 Kraków, Poland

The influence of the impurity substituted on the regular site in the BCC  $\alpha$ -Fe on charge and spin density on the adjacent iron nuclei has been studied by the *ab initio* method within framework of the full-potential linearized augmented plane-wave formalism applying density functional theorem. Results were correlated with the phenomenological cellular atomic model of Miedema and van der Woude and with the Mössbauer spectroscopy experimental data.

PACS: 75.50.Bb, 31.15.A-, 76.80.+y

## 1. Introduction

Impurity substituted on the regular iron site within BCC  $\alpha$ -Fe has influence on the charge (electron) density and electron spin density (hyperfine field) on the adjacent iron nuclei. One can study these effects by means of the <sup>57</sup>Fe Mössbauer spectroscopy. Namely, the average isomer shift (charge density) and hyperfine field varies with the impurity concentration for random distribution of impurities. Additionally, one can see individual effect of impurities to the second and sometimes to the third co-ordination shell. Hence, the impurity has effect on the average isomer shift  $\langle S \rangle$ , while individual perturbations to the particular impurity could be described as  $\Delta S_n$  with the index  $n$  denoting subsequent co-ordination shells around the resonant atom. Corresponding perturbations of the spin density influence the average hyperfine field  $\langle B \rangle$  and lead to the individual impurity effects  $\Delta B_n$  [1].

Parameters described above could be determined from the Mössbauer spectrum. Usually, one has to collect a series of spectra versus impurity concentration  $c$ . On the other hand, one can calculate electron density on the iron nucleus for single impurity — the latter located at various co-ordination shells around resonant atom. Similar calculations could be performed for the spin density, i.e., for the hyperfine field.

The phenomenological cellular atomic model (CAM) of alloys proposed by Miedema and van der Woude [2, 3] could be used to estimate the average isomer shift  $\langle S_M \rangle$  due to impurities, and to estimate contribution to the isomer shift caused by the impurity in the first co-ordination shell  $\Delta S_1^{(M)}$ . The model relies on the electro-chemical potential and electron density for the Fermi gas of non-interacting fermions.

This contribution concentrates on the correlations between experimental and/or calculated *ab initio* electron

and spin densities and similar quantities obtained within CAM model.

## 2. Discussion of results

Mössbauer data are partly taken from literature (Be [4], Al [5], Si [6], P [7], Ti [8], V [9], Cr [10], Mn [11], Co [12], Ni [11], Ge [13], As [14], Sn [15], Sb [14], W [16], Re [17], Pt [18]) or obtained in our laboratory (Cu [19], Zn [19], Ga [20], Nb [21], Mo [22], Ru [23], Rh [24], Pd [25], Os [26], Ir [27], Au [28]). Spectra obtained in our laboratory were processed by specialized program *Gmbernz* [21]. The latter program belongs to the MOSGRAF suite. *Ab initio* calculations of impurities in BCC-Fe were performed within the spin-polarized density functional theory (DFT). The pseudopotential method with the generalized gradient approximation (GGA) parameterized by Perdew–Burke–Ernzerhof method (PBE) as implemented in the VASP code [29] was used to optimize geometry and atomic positions of the 128-atomic super-cell. Atoms were represented by the projector-augmented wave pseudopotentials (PAWs) provided by VASP. A plane-wave expansion up to 360 eV was applied. The Brillouin zone of each super-cell containing a defect was sampled using the  $3 \times 3 \times 3$  k-point mesh generated by the Monkhorst–Pack scheme. During defect calculations, the lattice vectors of the super-cell were frozen at the GGA optimized value and the atomic positions were relaxed until the forces acting on all atoms of the super-cell were smaller than 0.01 eV/Å. The total energy was converged down to 0.1 meV/super-cell. Hyperfine parameters were calculated using the full-potential all electron plane wave method (FLAPW) as implemented in the WIEN2k code [30]. These calculations were carried out using the same exchange–correlation approximation and 4 k-points in the irreducible part of the Brillouin zone for the tetrahedron method of integration. The muffin-tin radii of particular atoms were set to conform criterion of the almost touching spheres. The cut-off energy expressed as the product of the muffin-tin radii

\* corresponding author; e-mail: [sfblacho@cyf-kr.edu.pl](mailto:sfblacho@cyf-kr.edu.pl)

and the maximum plane wave vector was equal to 7 and the largest reciprocal vector for the charge Fourier transfer amounted to 12 to guarantee the total energy convergence of the order of 0.01 mRy/super-cell.

Phenomenological CAM approach relies on the following empirical expression [2]:

$$S = A(\Phi_a - \Phi_b) + B \left( \frac{n_a - n_b}{n_b} \right) + S_b. \quad (1)$$

The symbol  $S$  denotes isomer shift observed for the alloy containing diluted impurities  $a$  in the matrix  $b$ . The isomer shift is observed on the resonant atoms belonging to the matrix  $b$ , while impurities  $a$  substitute matrix atoms at random. Symbols  $\Phi_a$  and  $\Phi_b$  denote respective electrochemical potentials of the pure elements forming binary alloy. Corresponding symbols  $n_a$  and  $n_b$  stand for densities of the electrons, the latter treated as non-interacting fermions. Electron density has to be expressed in the units of  $4.6 \times 10^{22} \text{ cm}^{-3}$  [2]. The symbol  $S_b$  stands for the isomer shift in the pure matrix. Finally, parameters  $A$  and  $B$  are to be adjusted basing on the experimental data. Electro-chemical potentials and electron densities relevant for the model are listed for various elements in Ref. [3]. Equation (1) was applied to: (a) the variation of the average isomer shift  $d\langle S \rangle/dc$  versus impurity concentration  $c$ , (b) the experimental first shell perturbation of the isomer shift  $\Delta S_1^{(E)}$  (averaged over impurity concentration) and (c) the *ab initio* calculated first shell perturbation of the isomer shift  $\Delta S_1^{(C)}$ . Above quantities were used instead of  $S$  in the Eq. (1). Details concerned with the determination of the average hyperfine parameters and  $\Delta S_1^{(E)}$  from the experimental Mössbauer spectra are described in [21]. Obtained values for the adjustable parameters  $A$  and  $B$  of CAM are listed in Table. These parameters were used to estimate respective parameters  $d\langle S_M \rangle/dc$  and  $\Delta S_1^{(M)}$  following from CAM. The last parameter  $\Delta S_1^{(M)}$  has been obtained for experimental data (b) and calculated data (c) — see Fig. 1. Parameters  $\Delta S_1^{(M)}$  calculated by using experimental input data for the Eq. (1) (case (b)) are slightly different while using *ab initio* calculated data as input of the Eq. (1) — case (c).

TABLE

Parameters (all  $\times 10^2$ ) of the CAM obtained for (a), (b) and (c) data sets. See text for details.

	$A$	$B$	Dispersion
(a)	0.79 mm/(s V at.%)	-2.11 mm/(s at.%)	0.20 mm/(s at.%)
	[mm/(s V)]	[mm/s]	[mm/s]
(b)	3.00	-11.18	2.60
(c)	4.86	-13.25	1.66

Figure 1a shows correlation between experiment and CAM model for  $d\langle S \rangle/dc$ . A correlation between experiment and CAM for the  $\Delta S_1$  (due to the first shell) is shown in part (b), while the corresponding correlation between *ab initio* results and CAM for  $\Delta S_1$  is shown in part (c).

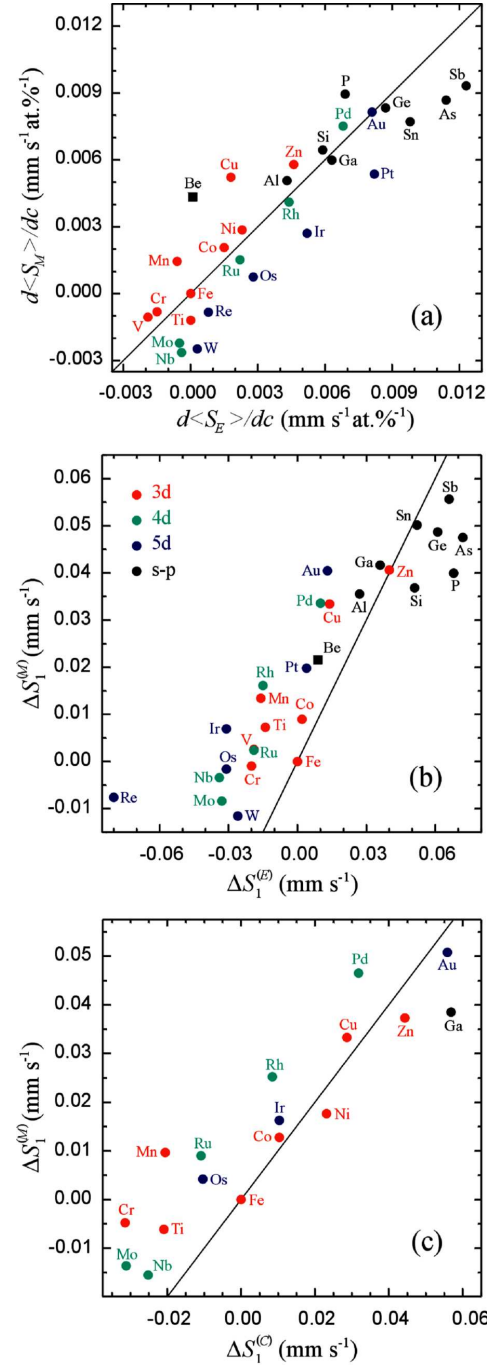


Fig. 1. (a) Correlation between experimental derivative  $d\langle S_E \rangle/dc$  of the isomer shift versus impurity concentration  $c$  and corresponding derivative within CAM model  $d\langle S_M \rangle/dc$ . (b) Correlation between experimental first shell perturbations of the isomer shift  $\Delta S_1^{(E)}$  and  $\Delta S_1^{(M)}$  obtained basing on the experimental data. (c) Correlation between calculated  $\Delta S_1^{(C)}$  and  $\Delta S_1^{(M)}$  obtained basing on the *ab initio* calculated data. Straight lines show “ideal” correlation.

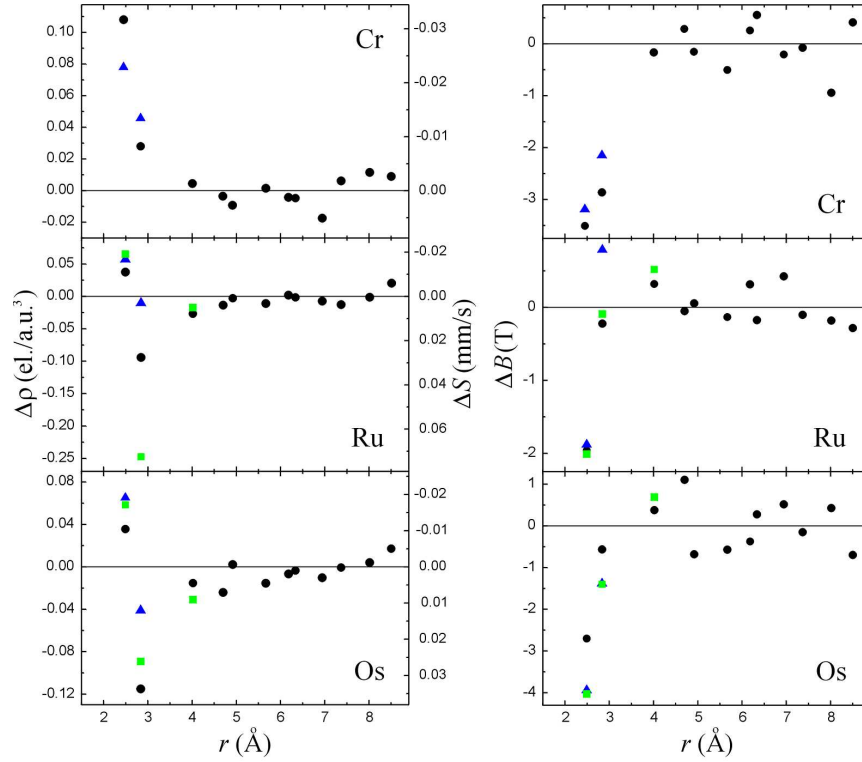


Fig. 2. Variation of the electron density  $\Delta\rho$  and corresponding isomer shift  $\Delta S$  versus distance  $r$  from the impurity (co-ordination shell). Right column shows corresponding variation of the hyperfine field  $\Delta B$ . Results of the *ab initio* calculations are shown for Cr, Ru and Os. Blue triangles denote experimental data processed to the second co-ordination shell, green rectangles correspond to the experimental data processed to the third shell [10, 23, 26], while black circles are outcome of the *ab initio* calculations.

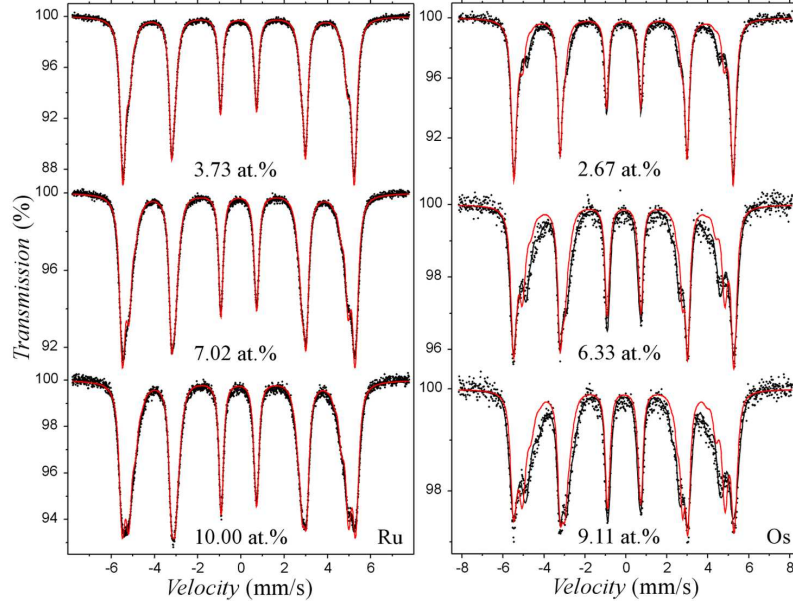


Fig. 3. Mössbauer spectra obtained for various concentrations of Ru and Os. Red lines correspond to the perturbations of the charge and spin density obtained from the *ab initio* calculations.

Figure 2 shows selected results of the *ab initio* calculations. Namely, the variation of the electron density versus distance  $r$  from the impurity is shown for

Cr, Ru and Os. The electron density variation  $\Delta\rho$  is taken relative to the density due to the distant impurity. The variation of the electron density is re-scaled to

the variation of the isomer shift  $\Delta S$  by using calibration constant  $-0.291 \text{ a.u.}^3 \text{mm s}^{-1}$  [31]. Similar variation  $\Delta B$  for the hyperfine field is shown as well. Results of *ab initio* calculations for all d impurities soluble in  $\alpha$ -Fe are to be published separately, soon.

Figure 3 shows selected spectra for various concentrations of Ru and Os in iron. Black solid line is the result of fit by *Gmbernz* program, while the red line was obtained by means of the similar fit, albeit with the  $\Delta S_n$  and  $\Delta B_n$  ( $n = 1, 2, 3$ ) taken from the *ab initio* results.

### 3. Conclusions

It is surprising that such simple phenomenological model like CAM reproduces quite reasonably the average isomer shift. Perturbations due to the impurity in the first co-ordination shell are reproduced a bit poorer, but still reasonably. The volume effect (unaccounted for in the simple version of the CAM used here) is visible as the separation of lines in Fig. 1a describing 3d, 4d and 5d impurities, respectively. The volume effect could be easily taken into account, while performing *ab initio* calculations [32]. The positive values of the parameter  $A$  are caused by the effect of sucking electrons from iron by the impurity having positive potential against iron (the calibration constant for iron is negative [31]). Negative values of the parameter  $B$  are due to the same effect, i.e., to the increased electron density for impurities having higher density than iron.

*Ab initio* results show that the impurity is able to perturb electron and spin density to about third co-ordination shell. This result is consistent with the large body of the experimental data processed by *Gmbernz*. Oscillations of the charge and spin density around impurity are seen both in calculations and experiment — particularly for Ru and Os.

Spectra fitted basing on the *ab initio* results depart from the experimental data with the increasing impurity concentration. This fact is understandable as *ab initio* calculations were performed for the isolated impurity within large super-cell. Currently, it is practically impossible to perform reliable calculations for the random alloy except for the very diluted limit. The number of configurations to be taken into account for the more concentrated alloy prevents detailed calculations.

### Acknowledgments

Professor Krzysztof Ruebenbauer, Pedagogical University, Kraków, Poland is thanked for contribution to the data evaluation and models development. Dr. Jan Żukrowski, AGH University of Science and Technology, Kraków, Poland is thanked for alloys preparation.

### References

- [1] A. Błachowski, *Acta Phys. Pol. A* **114**, 1563 (2008).
- [2] A.R. Miedema, F. van der Woude, *Physica* **100B**, 145 (1980).
- [3] A.R. Miedema, *Physica B* **182**, 1 (1992).
- [4] I. Vincze, A.T. Aldred, *Solid State Commun.* **17**, 639 (1975).
- [5] S.M. Dubiel, W. Zinn, *Phys. Rev. B* **26**, 1574 (1982).
- [6] S.M. Dubiel, W. Zinn, *J. Magn. Magn. Mater.* **28**, 261 (1982).
- [7] S.M. Dubiel, *Phys. Rev. B* **48**, 4148 (1993).
- [8] J. Cieślak, S.M. Dubiel, *J. Alloys Compd.* **350**, 17 (2003).
- [9] S.M. Dubiel, W. Zinn, *J. Magn. Magn. Mater.* **37**, 237 (1983).
- [10] S.M. Dubiel, J. Żukrowski, *J. Magn. Magn. Mater.* **23**, 214 (1981).
- [11] I. Vincze, I.A. Campbell, *J. Phys. F: Met. Phys.* **3**, 647 (1973).
- [12] J. Chojcan, *Hyperfine Interact.* **156/157**, 523 (2004).
- [13] S.M. Dubiel, W. Zinn, *Phys. Rev. B* **28**, 67 (1983).
- [14] I. Vincze, A.T. Aldred, *Phys. Rev. B* **9**, 3845 (1974).
- [15] S.M. Dubiel, W. Znamirovski, *Hyperfine Interact.* **9**, 477 (1981).
- [16] S.M. Dubiel, W. Zinn, *Phys. Rev. B* **30**, 3783 (1984).
- [17] S.M. Dubiel, *J. Magn. Magn. Mater.* **69**, 206 (1987).
- [18] S.M. Dubiel, *Phys. Rev. B* **37**, 1429 (1988).
- [19] A. Błachowski *et al.* – unpublished.
- [20] A. Błachowski, K. Ruebenbauer, J. Żukrowski, J. Przewoźnik, *J. Alloys Compd.* **455**, 47 (2008).
- [21] A. Błachowski, K. Ruebenbauer, J. Żukrowski, *Phys. Status Solidi B* **242**, 3201 (2005).
- [22] A. Błachowski, K. Ruebenbauer, J. Żukrowski, J. Przewoźnik, *J. Alloys Compd.* **482**, 23 (2009).
- [23] A. Błachowski, K. Ruebenbauer, J. Żukrowski, *Phys. Rev. B* **73**, 104423 (2006).
- [24] A. Błachowski, K. Ruebenbauer, J. Żukrowski, *J. Alloys Compd.* **477**, 4 (2009).
- [25] A. Błachowski, K. Ruebenbauer, J. Żukrowski, *Phys. Scr.* **70**, 368 (2004).
- [26] A. Błachowski, K. Ruebenbauer, J. Żukrowski, *Nukleonika* **49**, S67 (2004).
- [27] A. Błachowski, K. Ruebenbauer, J. Żukrowski, *J. Alloys Compd.* **464**, 13 (2008).
- [28] A. Błachowski, K. Ruebenbauer, J. Przewoźnik, J. Żukrowski, *J. Alloys Compd.* **458**, 96 (2008).
- [29] G. Kresse, J. Furthmüller, *Computer code VASP*, <http://cms.mpi.univie.ac.at/vasp/>; G. Kresse, J. Furthmüller, *Phys. Rev. B* **54**, 11169 (1996).
- [30] P. Blaha, K. Schwarz, G.K.H. Madsen, K. Kvasnicka, J. Luitz, *Computer code WIEN2k*, <http://www.wien2k.at>; K. Schwarz, P. Blaha, G.K.H. Madsen, *Comput. Phys. Commun.* **147**, 71 (2002).
- [31] U.D. Wdowik, K. Ruebenbauer, *Phys. Rev. B* **76**, 155118 (2007).
- [32] A. Błachowski, U.D. Wdowik, K. Ruebenbauer, *J. Alloys Compd.* **485**, 36 (2009).